Coherent dipole transport in a small grid of Rydberg atoms

Hui Yu[1] and F. Robicheaux[1,2,*]

[1]*Department of Physics and Astronomy, Purdue University, West Lafayette, Indiana 47907, USA*
[2]*Purdue Quantum Center, Purdue University, West Lafayette, Indiana 47907, USA*

We calculated the motion of one or two excitons through a small grid of Rydberg atoms. Both one- and two-dimensional grids were studied with the number of sites in a direction between 4 and 10. To mimic the possibility of nonperfect filling, calculations were performed with atoms randomly missing from sites. Results are presented for four qualitatively different situations. (1) The corners and edges, with the randomness of nonperfect filling, strongly affects the exciton motion and can pin the exciton. (2) For the case where a single exciton is simultaneously generated at two sites, the direction in which the exciton moves can be controlled by imprinting a phase difference on the two adjacent sites. (3) For the case where two excitons are generated at adjacent sites, calculations where a pair of excitons move through the grid are compared to the one exciton case to see whether exciton-exciton correlations are measurable. (4) The grid version of an exciton current can be defined by analogy to a continuity equation in one dimension and by using the analogy to a velocity operator in one, two, or three dimensions; for one dimension, the two definitions give similar results which means the direct measurement of the current in one dimension is possible.

I. INTRODUCTION

The transport of particles or energy or charge or spin, etc. through a system has been of fundamental interest in science from the earliest investigations through today. Transport necessarily involves the coupling between spatially separated regions of the system and the specific behavior of the transport is determined by the coupling. In this paper, we investigate the motion of an excitation (exciton) through a small grid of Rydberg atoms where the coupling is due to the $1/R^3$ dipole-dipole interaction between states on atoms separated by a distance R. Unlike our recent study [1] where we focused on randomness in systems of several tens of thousands of atoms, we will investigate how an exciton moves through a small grid of Rydberg atoms, often less than 10 atoms total. For an experimental realization, the only condition necessary is for one atom or a couple of atoms to be in a Rydberg state with angular momentum ℓ with the others being in a state with angular momentum differing by one, i.e., $\ell \pm 1$. We treat the case where one atom is (or a couple of atoms are) in a Rydberg p state and all of the others are in a Rydberg s state. The dipole-dipole interaction allows the p character to hop from atom to atom.

The idea of Rydberg excitations hopping through a (nearly) frozen gas of atoms goes back to the original experiments on Rydberg gases [2,3] where a dense gas of Rydberg atoms led to some states changing character. After changing character, the excitations could hop through the "sea" of excited states. Since the Rydberg states were generated from a gas of randomly placed atoms, the character of the exciton hopping was strongly affected by the random coupling between atoms. How an exciton hops through a completely random Rydberg gas was investigated in Refs. [4,5] with Ref. [5] showing that the exciton is typically trapped in a region of two or three atoms

in a random gas, which is consistent with the measurements in Ref. [6].

The interaction of a pair of atoms through the near-field form of the dipole-dipole interaction decreases with distance like $1/R^3$. The near-field form of the dipole-dipole interaction is appropriate because the energy difference between pairs of Rydberg states with principal quantum number n corresponds to frequencies of order $\omega \sim 1/n^3$; the wavelength of the light associated with this frequency is typically many orders of magnitude larger than the separation of the atoms and/or the total size of the system. The appropriateness of this approximation has been checked experimentally and can lead to different physical processes. For example, the dipole-dipole interaction can lead to the suppression of excitation in a gas and Ref. [7] observed the case where one atom prevented the excitation of more than 1000 atoms. References [8,9] observed this suppression between two individual atoms. The coherence of the dipole-dipole coupling between a pair of Rydberg atoms was investigated in Ref. [10]. Reference [11] provided spectroscopic evidence for the dipole-dipole interaction between cold Rydberg atoms. As a final example of basic phenomena, Ref. [12] gave experimental and theoretical evidence for spatially resolved observation of the effect of dipole-dipole interactions between Rydberg states and Ref. [13] measured the energy exchange between spatially separated Rydberg atoms.

All of the calculations in this paper have as the starting point a regular array of Rydberg atoms with a certain fraction of atoms randomly missing from sites. The exciton(s) will start at certain sites and the time evolution of the wave function will be coherent. We will not address how realistic this situation is but note that the necessary technology appears to be available. Reference [14] describes trapped Rydberg atoms in an optical lattice. Another method for creating a Rydberg array could start with atoms trapped in an optical lattice with a subsequent excitation to a Rydberg state. The calculations of Ref. [15] gave an optimal choice in laser parameters that could lead to Rydberg atoms being in a regular spatial array even though the

---

*robichf@purdue.edu

unexcited atoms are randomly distributed. On a similar note, Ref. [16] used polar molecules confined in an optical lattice to investigate the time evolution of coherently excited dipoles.

We only treat the case of one (or a couple) exciton(s) moving through a lattice. There have been several studies of the many-exciton case for Rydberg gases (e.g., see Refs. [17–22]), but the behavior of many excitons is beyond the scope of this paper. There have been several studies of exciton transport similar in spirit to the calculations presented here. Reference [23] considers an interesting case of using Rydberg dressing to effect transport of a more compact state. A similar system was studied in Ref. [24] but dissipation was introduced through coupling to states with short lifetimes. Reference [25] experimentally imaged the dipole-dipole-mediated transport of excitations between Rydberg atoms. The manifestation of excitation transport in the energy spectra of atoms interacting through the dipole-dipole term was numerically studied in Ref. [26]. We investigate the case of having the atoms placed on a lattice of sites with a specified amount of randomness in the fraction of sites with missing atoms. Within investigations using Rydberg atoms, Refs. [27,28] have addressed randomness within a lattice of atoms, up to six sites in Ref. [27] and two sites in Ref. [28]. Also, Refs. [4,5] investigated how an exciton hops through a completely random Rydberg gas. Lastly, Refs. [29,30] treated the case of exciton motion with "heavy-tailed disorder" in the diagonal elements of the Hamiltonian.

We perform calculations for the *coherent* transport of excitons through a lattice of Rydberg atoms. The exciton(s) start at specific sites and the wave function is propagated by using a Schrödinger equation in an effective-state basis set. Thus, the calculations should capture all of the interference effects that can lead to Anderson localization and represent a special case of interacting particles in a random potential [31]. Conversely, because we do not include any types of dissipation, the percolation or diffusive transport is not represented. All of the calculations are presented for perfect lattices, for lattices with 20% of the atoms randomly missing, and for lattices with 50% of the atoms randomly missing; while the missing atoms lead to a decrease in the average strength of the interaction, our results are not consistent with this being a dominant effect. The atoms are assumed to be frozen in space for the short time represented by the calculations. We focus on cases where there are relatively few atoms so that the effects of edges and/or corners become important. For example, Ref. [1] found that randomness in large two-dimensional arrays with wrapped boundary conditions did not lead to a large number of highly localized states. The results presented below show that an edge or corner in addition to the randomness will often lead to strongly localized states. Also, interesting interference patterns emerge during the exciton motion due to reflection from edges and corners. We also present calculations for the case where the motion of a single exciton can be guided if it can be split between adjacent sites with one site imprinted with a phase. For the type of exciton studied here, the motion is directed opposite to the phase increase (negative group velocity), as expected from the bands reported in Ref. [27]. In addition, we give two definitions of the exciton current (one that can be used only from experimental observables and one that requires the exciton wave function) and compare them for a simple line of

atoms. Finally, we present results for two coherent excitons and show that the restrictions on the exciton wave function leads to correlation even though there is no interaction between pairs of excitons.

Atomic units are used unless explicit SI units are given.

II. COMPUTATIONAL METHOD

For the calculations in this paper, we treat the case where one or two atoms have p-state character and the rest have s-state character. The dipole-dipole interaction is largest if the s and p states have a similar principal quantum number. For the cases treated in this paper, we chose the $30s$ and $30p$ states of Rb. The specific choice of angular momentum, n, and atom will affect the details of the exciton hopping but does not change the qualitative features.

The computational techniques are the same as in the part of Ref. [1] regarding the time-dependent calculations; these are Figs. 1, 3, 5, and 7 of Ref. [1]. The exciton(s) is (are) treated as a coherent quantum system. The atoms are assumed to be fixed in space over the relevant time scales and, thus, the character of the different atoms evolves through a quantum wave function

$$i\partial\Psi/\partial t = H\Psi, \tag{1}$$

where the Ψ contains the amplitudes for the different combination of states of each atom. We numerically solve this equation by using the leapfrog algorithm:

$$\Psi(t + \delta t) = \Psi(t - \delta t) - 2i\delta t H\Psi(t), \tag{2}$$

which has a one time step error of order δt^3. The leapfrog algorithm has two nice features when H is time independent: it exactly conserves the norm of Ψ and exactly conserves $\langle H^n \rangle$ with n an integer.

The special case discussed here (p-state coherent motion through a sea of s states) is treated as Eq. (6) in Ref. [27]. For one exciton, the basis states can be labeled as $|i,m\rangle$, meaning the p state is at site i with angular-momentum projection m. In this special case, the nonzero matrix elements reduce to

$$V_{im,i'm'} = -\sqrt{\frac{8\pi}{3}} \frac{(d_{n_a 1,n_b 0})^2}{R^3}$$
$$\times (-1)^{m'} \begin{pmatrix} 1 & 1 & 2 \\ m & -m' & m'-m \end{pmatrix} Y_{2,m'-m}(\hat{R}), \tag{3}$$

where the $d_{n_a 1,n_b 0}$ is the reduced matrix element between the p state with principal quantum number n_a and the s state with principal quantum number n_b, $(\ldots)$ is the usual 3-j coefficient and $\vec{R} = \vec{r}_i - \vec{r}_{i'}$ is the displacement vector between sites i and i'. For two excitons, the basis states can be labeled as $|i_1,m_1;i_2,m_2\rangle$ with $i_2 > i_1$.

For the general case, the nonzero matrix elements are complex. In order to treat the largest number of atoms, we further restricted the p state to have $m = 0$. This can be accomplished experimentally by having an external field so that the $m = 0, 1, -1$ states are sufficiently separated in energy so that the motion does not mix m. Now the basis state can be designated solely by the site i and the nonzero matrix elements reduce to

$$H_{ii'} = V_{ii'} = -\frac{2}{3} P_2(\cos\theta_{ii'}) \frac{(d_{n_a 1,n_b 0})^2}{R^3}, \tag{4}$$

where $P_2(x) = (3x^2 - 1)/2$ is a Legendre polynomial and $\cos\theta_{ii'} = (z_i - z_{i'})/R$. This expression is only for $i \neq i'$; when $i = i'$, the matrix element is 0: $H_{ii} = 0$. For the two-exciton case, the nonzero matrix elements reduce to

$$H_{i_1 i_2, i'_1 i'_2} = \sum_{a=1}^{2} \sum_{b=1}^{2} H_{i_a, i'_b} \delta_{i_{3-a}, i'_{3-b}}, \qquad (5)$$

where the one-exciton operator is from Eq. (4). If there are N atoms, there are N one-exciton states and $N(N-1)/2$ two-exciton states.

For atoms in a two-dimensional grid, the number of atoms scales as $N = N_1^2$ with N_1 being the number of sites in one direction; the number of two-exciton states for a two-dimensional grid is $N(N-1)/2 \simeq N_1^4/2$. The number of operations in one time step of Eq. (2) is from a matrix-vector multiply, $H\Psi$, and is proportional to the square of the number of states. Thus, the number of operations involved in one time step for the two-exciton problem in two dimensions scales like N_1^8. Thus, the two-exciton calculations can transition from computationally easy to "impossibly" long over a small range of N_1.

For the calculations with nonperfect filling, the results were obtained by averaging over many different random configurations. Each configuration was constructed by using a random number generator to randomly decide whether or not a site was occupied by a Rydberg atom. Thus, the number of atoms in any run fluctuated with each configuration. If there was no atom at the initial site of an exciton, then that configuration was not used. If there was an atom at the initial site of every exciton, then the Eq. (2) was solved and the probability for an exciton to be at each site was stored and averaged over many configurations. This mimics the way an experiment would work if performed with destructive measurement of the exciton position.

III. RESULTS

In all of our calculations, we use the $30s$ and $30p$ states of Rb as our sea and excitation states, respectively. The size of these states is less than 0.1 μm. The standard step distance between atoms will be 10 μm. Thus, the interactions of higher order than dipole-dipole are negligible. These states have dipole matrix element $d_{30s,30p} = 846$ a.u.; this value was obtained by using the numerical method described in Ref. [32] but based on the updated quantum defects in Ref. [33]. For the one- and two-dimensional calculations, the atoms will be confined in the xy plane, which means there is no angular dependence to the matrix elements coupling different states.

A useful quantity is the energy scale of the matrix element between nearest neighbors: $E_{sc} \sim d^2/R^3 = 1.06 \times 10^{-10}$ a.u. We can convert this to a timescale by $t_{sc} = 2\pi/E_{sc} = 5.93 \times 10^{10}$ a.u. which is 1.43 μs. This gives a sense of the timescale needed for the p state character to move from site to site. The Hamiltonian can be scaled in terms of d^2/R^3, which means our results can be scaled in a similar way. For example, the timescale is decreased by a factor of four if the dipole matrix element is a factor of two larger; the timescale is decreased by a factor of eight if the separation between atoms is a factor of two smaller.
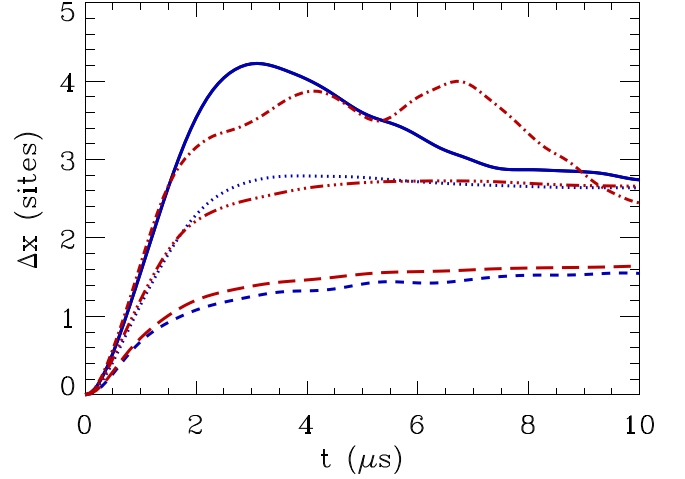
FIG. 1. The average number of sites for the p state to have moved in the x direction when the exciton starts at the lower-left corner of a two-dimensional array (blue) or at the center of the left edge of the array (red). The array has 7×7 possible sites. For the corner initial position, the solid line is for 0% missing atoms, the dotted line is for 20% missing atoms, and the short-dash line is for 50% missing atoms. For the "center of left edge" initial position, the dash-dot line is for 0% missing atoms, the dash-dot-dot-dot line is for 20% missing, and the long-dash line is for 50% missing.

A. One exciton starting at a corner or edge

In this section, we present the results of calculations where the wave function has a single exciton that initially is at a corner or an edge position. For all of the calculations, we show the results for a 7×7 array of atoms, although the 5×5 and 9×9 arrays showed similar results.

Figure 1 shows the average distance the exciton has hopped in the x direction divided by the distance between adjacent sites. Results are shown when the exciton starts at the lower-left corner of the array and for when it starts at the center of the left edge of the array. The ordinate of Fig. 1 can be thought of as the average number of sites the exciton has moved in the x direction. By symmetry, the average distance hopped in the y direction will be the same as the x direction for a corner start. For the center-edge initial position, the average distance hopped in the y direction is 0 by symmetry.

Some of the general features should be expected. For example, as the fraction of missing atoms increase, the distance the exciton hops at early times decreases. This arises because missing sites mean the exciton must hop further to reach the next atom. However, the decrease is not simply due to the decrease in the interaction strength but is more due to a missing site blocking the motion of the exciton. If Δx is divided by the fraction of missing sites, then all of the curves are approximately the same for times less then $\simeq 1$ μs. This scaling would not result if the time was scaled by the average decrease in coupling, d^2/R^3, but does result if the early-time motion to the next site is blocked a fraction of the time. Also, it might be expected that a perfect array will lead to the exciton hopping quickly to the other side of the array with something like ballistic transport but with substantial spreading due to the highly localized initial state; thus, the solid and the dash-dot lines show an early-time peak of ~ 4 sites.

Perhaps surprisingly, the early-time behavior ($t < 1.5 \ \mu s$) of the exciton does not show a strong effect on whether the exciton starts in a corner or at an edge. The early-time increase in Δx is very similar even though the corner start is effectively missing atoms below it. This result is due to the fact that the early-time behavior of Δx is only determined by the presence or absence of atoms immediately to the right of the starting position. For the exciton to hop up or down and then right (which is available for an edge start but not down for a corner start) requires a longer time and shows up later in the graph.

For the case with missing atoms, the long-time behavior of the hopping seems to lead to a finite size Δx noticeably less than the average for the array, which is three. As the randomness increases from 20% to 50%, it is not surprising that the average hopping distance decreases. However, it is somewhat surprising that the hopping distance is so small. From Ref. [1], it seems that there is not a large amount of localization in two dimensions (for example, see Figs. 5 and 6 of Ref. [1]) even for a large amount of randomness. This was explained as being due to the many paths an exciton can take through a two-dimensional (2D) lattice even when many sites are missing atoms. However, Fig. 1 for 50% missing has an average hopping distance of ~ 1.5 sites at late times, which indicates most excitons are pinned within one or two sites of the edge. The small hopping distance in Fig. 1 is due to the additional "defect" from the edge of the lattice itself which helps to pin the exciton compared to the calculations of Ref. [1] where there were no edges. Finally, it is not surprising that the late-time value of Δx does not depend on the starting position since the exciton will move in y as well so that the initial y position will not be so important.

Figure 2 shows the probability that the exciton is in the column with site x at different times when the exciton starts in the lower-left corner of the array. As above, these results are for a 7×7 array but similar-size arrays give a similar result. The results in this figure correspond to 50% filling of the sites. At $t = 0$, the probability to have $x = 1$ is 1. Even before the scale time of $t_{sc} \sim 1.4 \ \mu s$ is reached, the exciton has substantial population in the columns two and three at 1 μs. By 2 μs, the population in each column has nearly reached the late-time value with the main exception being the farthest: columns five to seven. Note that, even at the latest time, there is only a population of $\simeq 1/20$ in column seven compared with a roughly statistical value of $\simeq 1/7$ for the case with no missing atoms. This figure shows that an experiment would not need substantial delays to obtain the late-time distribution of an exciton if there is a large fraction of missing atoms. It also shows that the exciton is somewhat pinned to the left edge of the array with $\sim 3/4$ of the population in columns one to three.
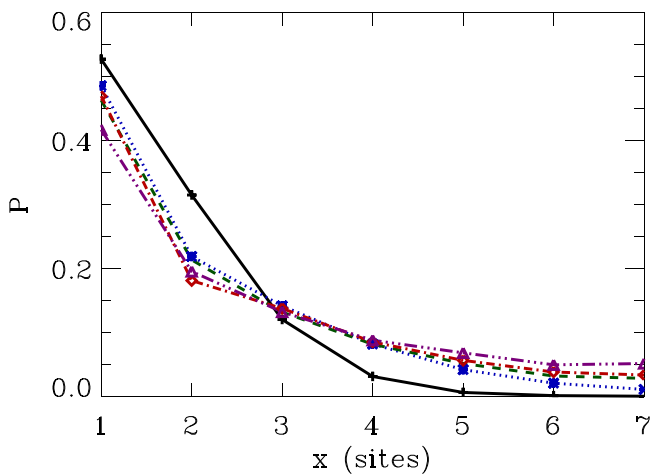
Figure 3 shows the 2D probability for the exciton to be at different positions after 2 μs when starting at the middle of the left edge. The different filling probabilities are 0% missing [Fig. 3(a)], 20% missing [Fig. 3(b)], and 50% missing [Fig. 3(c)]. From Fig. 3(c), it is clear that the exciton does not move far during this time when 50% of the sites are missing; even in Fig. 3(b), there is a substantial population still at the initial site while there is very little remaining at the initial site for perfect filling. This is another indication that the edge *plus* randomness can pin the exciton. Figures 3(a) and 3(b) show an interesting feature: the highest probability is for the exciton to be either above or below the initial position. For the 0% missing case, the highest probability is at the upper and lower edges of the array. For the 20% missing case, the highest probability is for the exciton to remain in place. However, the next highest probabilities are at the $(x,y) = (2, 4 \pm 2)$ sites (i.e., shifted to the right by one site and up or down by two sites).

B. One exciton: coherent superposition of two sites

In Ref. [27] is a discussion of the band structure of an exciton that hops by using the dipole-dipole interaction (see Figs. 2, 3, and 4 for one-, two-, and three-dimensional arrays). Although the bands are an infinite, perfect lattice property, there are features of the bands that are manifest in finite, imperfect arrays. One of the simplest properties is the transport of an exciton when adjacent sites are given different phases.

We performed calculations for one exciton with an initial wave function that was the coherent superposition of two sites. One can choose the sites to mimic various directions in $\vec{k}$. As an illustration, we chose to have $\vec{k}$ to be in the x direction. The wave function at $t = 0$ had the form $\Psi(0) = [|i_x, i_y\rangle + \exp(i\phi)|i_x + 1, i_y\rangle]/\sqrt{2}$ where $|i_x, i_y\rangle$ indicates the exciton is at the site (i_x, i_y). For small positive ϕ, the wave function mostly projects onto states with positive k_x. As ϕ increases, the average k_x also increases.

Figure 4 shows results for a perfect 6×6 lattice where the exciton is started with the mixture $[|3,3\rangle + \exp(i\phi)|4,3\rangle]/\sqrt{2}$. The plot shows how far the exciton moves from its initial expectation value of $\langle x \rangle(0) = 3.5$ in units of sites. The different curves correspond to different values for ϕ. There is only one curve for negative ϕ because the Δx changes sign if ϕ changes sign for the symmetric starting condition in this figure.

The initial change in position with respect to time is positive for negative values of ϕ (and, hence, negative k_x) and is negative for positive values of ϕ. This may be the opposite

FIG. 2. Same arrangement as Fig. 1 for 50% filling. The probability for the exciton to be in the column with site x at different times: solid (1 μs), dotted (2 μs), dashed (3 μs), dot-dash (4 μs), and dash-dot-dot-dot (10 μs). $x = 1$ is the leftmost edge of the array and $x = 7$ is the rightmost edge. At $t = 0$, the exciton is in the lower-left corner of the array.
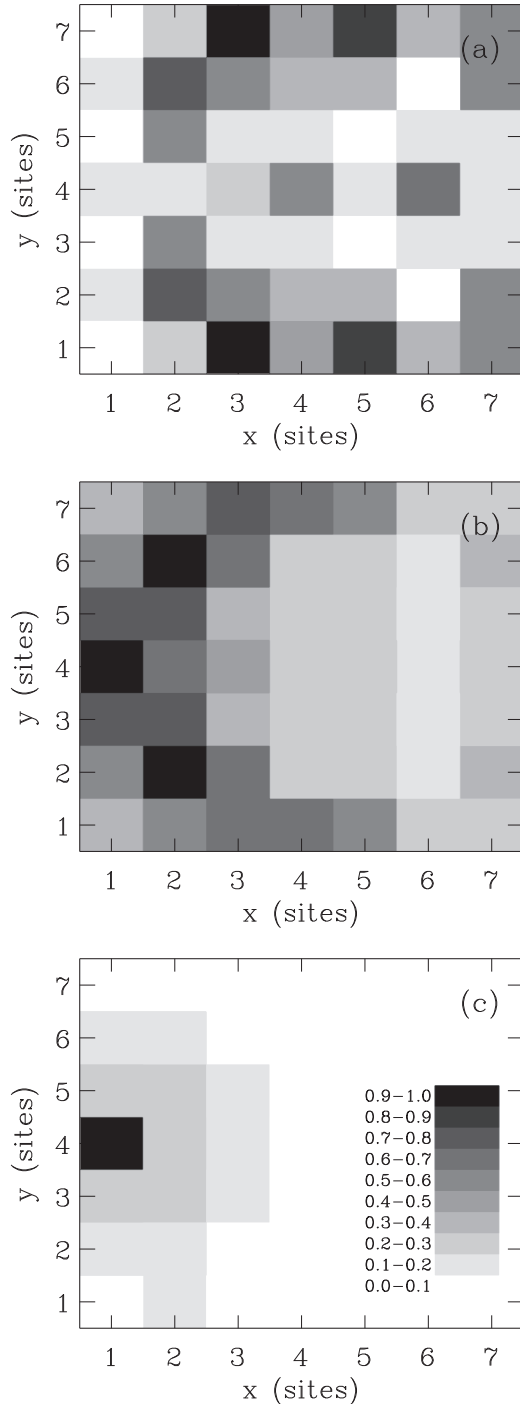
FIG. 3. Same arrangement as Fig. 1. The probability (with arbitrary normalization) for the exciton to be at different sites at $t = 2$ μs for (a) 0% missing, (b) 20% missing, and (c) 50% missing. The different shades represent a linear decrease in probability. The initial position of the exciton is at the middle of the left edge: $x = 1$, $y = 4$. The legend in panel (c) is for all figures.

of what a casual reader expects but it agrees with the results plotted in Fig. 3 of Ref. [27]. The case where the p orbital is oriented out of the plane corresponds to the band that starts at $\epsilon \simeq 1$ at $k = 0$ and decreases from that value. A band with a decreasing ϵ versus k corresponds to a negative group velocity.
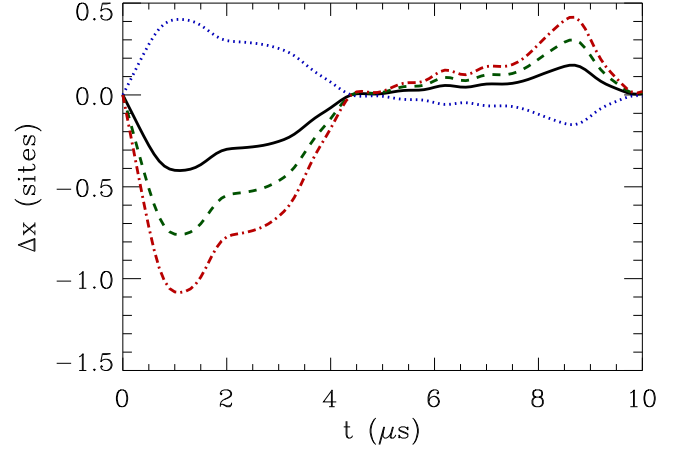
FIG. 4. Similar to Fig. 1 but with different array size and initial conditions. The change in the average x for an exciton coherently excited at neighboring sites for a 6×6 array with 0% missing. The two sites $(x,y) = (3,3)$ and $(4,3)$ are equally excited with the latter site having phase ϕ relative to the first. The solid line is for $\phi = \pi/8$, the dotted lie is for $\phi = -\pi/8$, the short dashed line is for $\phi = \pi/4$, and the dash-dot line is for $\phi = \pi/2$.

At later times (starting ~ 1 μs), the exciton reflects off of the lattice edge and starts to move in the opposite direction.

Although the results are not presented in this paper, we also performed calculations for randomly missing sites. The results are similar to those presented in previous sections. The results for 20% missing have the same generic behavior as in Fig. 4 but the average Δx does not increase or decrease as rapidly as the perfect-lattice case; also, the largest change in position is not as big as for the perfect lattice. The results for 50% missing have even smaller contrast than the 20% missing case.

The results of Fig. 4 show that there can be considerable control over the exciton motion even starting with only a two-site coherence. If there were different angular momenta and/or polarization of the exciton, the band character can substantially change. Thus, measuring how the exciton moves when started with two-site coherence, even in a small grid of Rydberg atoms, will give insight into the exciton band(s).

C. Definition of probability current

The probability current $\vec{J}$ is defined as $\vec{J} = (\hbar/[2Mi])[\Psi^*\vec{\nabla}\Psi - \Psi\vec{\nabla}\Psi^*]$ for a particle moving through space. This definition is derived from the Schrödinger equation in nearly all textbooks on quantum mechanics (see, e.g., problem 1.14 of Ref. [34]). This definition is not applicable for the exciton hopping through a lattice due to the discreteness of the exciton position. However, the instantaneous current density could be an interesting quantity for the hopping exciton because it gives insight into the motion at a particular time: a given density at time t, $\rho = \Psi^*\Psi$, does not determine J. For example, $\Psi \propto \exp(ikx - \alpha x^2)$ gives the same ρ independent of k while $\vec{J}$ is proportional to k. Although this definition of probability current cannot be applied for the exciton hopping through the finite lattices, the current density can be generalized by using a velocity operator defined as

$$\vec{v} \equiv -i(\vec{r}H - H\vec{r}). \qquad (6)$$

For the exciton Hamiltonian of Eq. (4), the x component of the velocity operator is

$$(v_x)_{jj'} = -i(x_j - x_{j'})H_{jj'}, \tag{7}$$

and the x component of the current density can be defined as

$$(J_x)_j = \text{Re}\left[\psi_j^* \sum_{j'} v_{jj'}\psi_{j'}\right], \tag{8}$$

where j is the index that specifies the lattice site of the exciton. This definition presumes the knowledge of the wave function at all sites and can only be extracted from calculations.

For the one-dimensional case, it is possible to define a current density that only uses the time derivative of the probability for the exciton to be on each site. This definition is of interest because it can be implemented in an experiment to show the flow of exciton probability. We artificially expand the grid for the exciton to be extended from the sites $1 - N$ to the sites $0 - (N + 1)$ but the probability for the exciton to be at sites 0 or $N + 1$ is always 0. For the definition of the current density, we define the J_x to be at the half-integer grid $1/2, 3/2, \ldots, N + 1/2$. Since the exciton sites 0 and $N + 1$ always have 0 probability, we define the current density at the $1/2$ and $N + 1/2$ sites to be 0 because the population of excitons at sites 0 and $N + 1$ do not change with time. For all other sites, we define

$$\frac{d\rho(i_x,t)}{dt} \equiv -[J_x(i_x + 1/2,t) - J_x(i_x - 1/2,t)], \tag{9}$$

where $\rho(i_x,t) = |\Psi(i_x,t)|^2$ is the probability for the exciton to be at site i_x at time t. The right-hand side is a definition of how the current changes if the probability is restricted to local hopping. This is not the case when sites beyond nearest neighbor can contribute to the exciton motion. However, this definition will allow for a qualitative picture of the flow of the exciton through the lattice.

The case of a line of six atoms is shown in Fig. 5 for a different fraction of missing atoms. The exciton is started at the first x site. The two definitions, Eqs. (8) and (9), give similar currents for the times shown even though they are based on completely different definitions. Thus, even though the definition in Eq. (9) is only qualitatively relevant, the resulting current densities give information about how the exciton moves through the lattice of atoms. The definition of J means the current at site $1/2$ is exactly 0 at all times. Conservation of norm means the current is also exactly 0 at all times for site $N + 1/2$.

There are qualitative features for this specific example that highlights some of the physics processes. At 1 μs, the largest current is for the case of 0% missing atoms and is smallest for 50% missing atoms. This matches the expectation that the exciton moves most easily through a perfect lattice. For 0% missing atoms, the exciton moves to larger x for 1 and 2 μs and reflects off the lattice edge and moves to smaller x for 3 μs. This is seen in the current which is positive and moving to the right for 1 and 2 μs but is negative (indicating motion to the left) and peaked near the end of the lattice at 3 μs. One nontrivial feature is that the current for both the 20% and 50% missing sites are noticeably negative at small x for 2 μs. This feature is from the reflection of the exciton off
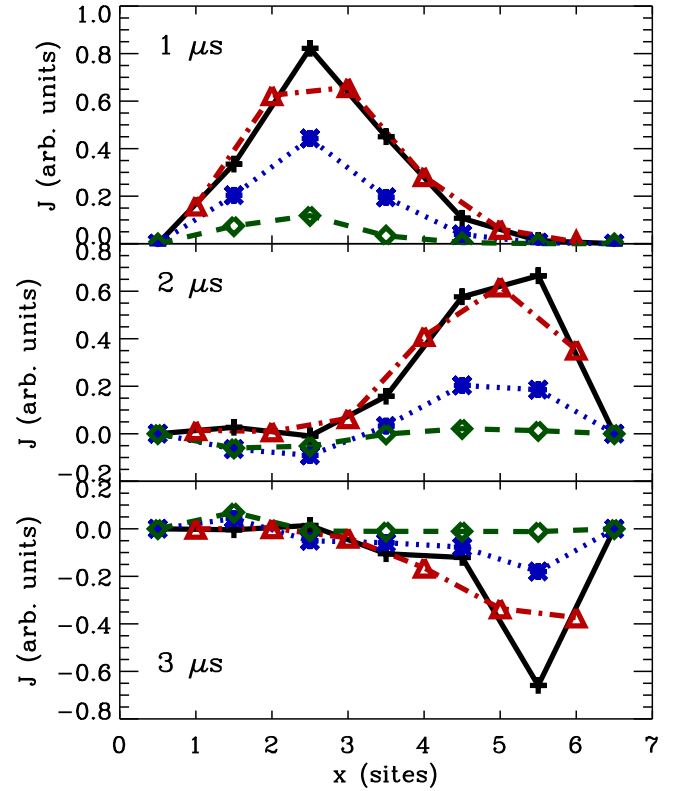
FIG. 5. The current density defined in Eq. (9) for a line of six atoms at three different times. For the definition of Eq. (8), the current is only defined at the sites; the line is to guide the eye. The dash-dot line (triangles) is the case of 0% missing atoms. For the definition of Eq. (9), the current is only defined on the half-integer points; the lines are to guide the eye. The exciton is started at the first x site. The case of 0% missing is the solid line (plus signs), the 20% missing is the dotted line (crosses), and the 50% missing is the dashed line (diamonds). All curves have been scaled by the same factor.

missing sites which gives a left-moving population at early times. This reflection from missing sites leads to population reflecting from the left edge of the lattice at 3 μs which gives a noticeable positive current at small x at that time.

The one-dimensional current, Eq. (8), can be easily generalized to two or three dimensions. However, there is not enough information in $d\rho(i_x,i_y,t)/dt$ to constrain a definition of a vector current $J_x(i_x,i_y,t)$ and $J_y(i_x,i_y,t)$ similar to Eq. (9) since there are $2(N - 1)N$ unknowns and only $N^2 - 1$ independent equations. However, integrals along a line of atoms can give the total current in the x or y direction. For example, in Eq. (9), the density can be generalized to $\rho(i_x,t) \equiv \sum_{i_y} \rho(i_x,i_y,t)$. This could lead to some insight into how the exciton hops through two-dimensional arrays.

D. Two coherent excitons

Although two excitons do not directly interact with each other, the restrictions on the wave function lead to an effective interaction which cannot be neglected when there are two or more excitons hopping through the lattice. This can be seen in the simplest case of two excitons. The wave function can be expressed as the amplitude for one exciton to be at site j_1 and the other exciton to be at site j_2: ψ_{j_1,j_2}. Since

the exciton is simply the existence of a p state at a certain site, there cannot be terms in the wave function corresponding to $j_1 = j_2$. Also, j_1, j_2 is indistinguishable from j_2, j_1. Thus, we artificially order the sites and restrict $j_1 < j_2$. Thus, this system is similar to a Hubbard model with infinite onsite interaction or a Tonks–Girardeau gas on a lattice. The main difference is that the long-range nature of the hopping allows the exciton combination to directly hop from $j_1 < j_2$ to $j_1' > j_2$. This calculation is a special case of two particles coherently hopping in a random potential [31]; it may be worth pursuing calculations of this system to much larger sizes to understand the asymptotic localization properties.

To have the strongest possible effect from two excitons, a higher density of excitons is important. Unfortunately, this requirement is in conflict with having a reasonable range of sites for the excitons to hop. In two dimensions, even several atoms in each direction (e.g., 6×6) will lead to the excitons rarely finding each other. To increase the effect of having a second exciton, we focus on the case of one dimension and start the excitons at adjacent sites.

The results in Fig. 6 show how the separation of two excitons behave in a one-dimensional lattice. The expectation value of the separation is calculated from

$$\Delta x = \sum_{j_1 < j_2} (j_2 - j_1) |\psi_{j_1 j_2}|^2, \tag{10}$$

where the calculations with missing atoms include a subsequent averaging over the different configurations of missing atoms. The situation for Fig. 6 starts the excitons in sites one and two of the lattice. To contrast with independent excitons, we performed calculations for two different initial positions of the excitons using exactly the same atomic arrangements as for the two-exciton calculations. For the uncorrelated excitons,
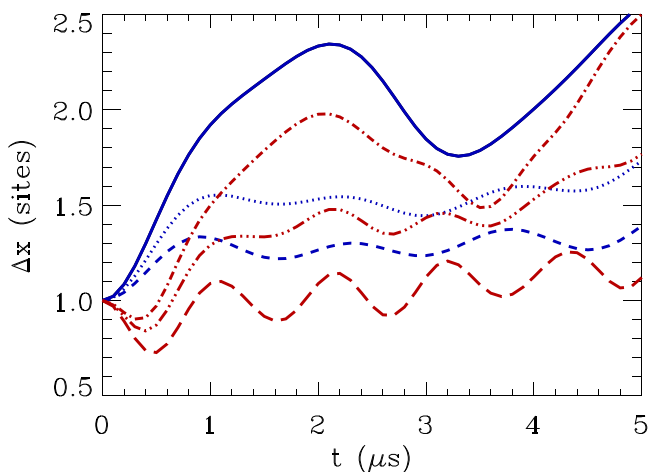
FIG. 6. The expectation value of the separation of two excitons in a one-dimensional line of seven atoms. The excitons start at sites one and two. The calculations for two-exciton hopping are for 0% missing atoms (solid line), 20% missing atoms (dotted line), and 50% missing atoms (short-dashed line). The calculations for two independent one-exciton calculations are for 0% missing atoms (dash-dot line), 20% missing atoms (dot-dot-dot-dash line), and 50% missing atoms (long-dash lines).

we calculated the expectation value of the separation from

$$\Delta x = \sum_{j_1, j_2} |j_2 - j_1| \big|\psi_{j_1}^{(1)}\big|^2 \big|\psi_{j_2}^{(2)}\big|^2, \tag{11}$$

where $\psi^{(k)}$ starts with the exciton initially at site k.

One clear difference between the calculations is the fact that $\Delta x \geqslant 1$ for all times for the two-exciton calculation while Δx can be less than one for the uncorrelated calculation. The reason is that the closest two excitons can be in the correlated calculation is a one-site separation which means the expectation value will always be larger than or equal to one. However, in the uncorrelated calculation, the probability the two excitons are on the same site is not 0 and, in fact, all calculations lead to an initial decrease in Δx from 1 as both excitons spread into overlapping sites. Another important difference is that the separation is larger for almost all times in the full calculation compared with the uncorrelated calculation. This means there is an effective repulsive interaction between the excitons at early times that leads to an increase in separation. However, there are some similarities between the correlated and uncorrelated calculations that indicate that some aspects of the exciton hopping is included in the uncorrelated calculation. For example, the case of 0% missing sites (solid line for correlated and dash-dot line for uncorrelated) shows an initial rise through ~ 2 μs, followed by a decrease through ~ 3.2 μs, with a subsequent increase through ~ 5 μs.

IV. CONCLUSIONS

We performed calculations for excitons coherently hopping through small lattices. Unlike the results in Ref. [1] which were for the largest computationally accessible lattices, the small lattice leads to new effects arising from the corners and edges of the lattice. For example, it seems that a corner or an edge can lead to strongly localized excitons when there are other randomly missing sites. Also, starting the excitons at particular spots can lead to interesting patterns in the transport that arises from reflections at edges and corners. For example, starting the exciton at the center of an edge can lead to population mostly localized at the sides of the lattice at particular times. Also, imprinting a phase on an exciton evenly divided between adjacent sites can lead to directional motion even for small lattices. For the type of exciton investigated here, the direction of motion is opposite that of the phase increase, i.e., the exciton has negative group velocity.

The exciton current density has not been previously investigated for Rydberg gases. Calculations were performed for two possible definitions of exciton current density: one definition requires the wave function and is, thus, only accessible to calculation while the other definition could be used in an experiment. The two definitions provided similar results for the case of an exciton hopping through a line of atoms.

Calculations were also performed for a two-exciton system and compared to that of two uncorrelated excitons with the same initial conditions. For a line of atoms, the exciton Hamiltonian is similar to a Hubbard model with infinite onsite interaction or a Tonks–Girardeau gas on a lattice with

important differences arising from the long-range nature of the exciton hopping. For the cases investigated, the two-exciton calculation demonstrated both striking differences and similarities to the uncorrelated calculation. The two- (or more) exciton case probably deserves a more in-depth treatment than given here.

[1] F. Robicheaux and N. M. Gill, Phys. Rev. A **89**, 053429 (2014).

[2] W. R. Anderson, J. R. Veale, and T. F. Gallagher, Phys. Rev. Lett. **80**, 249 (1998).

[3] I. Mourachko, D. Comparat, F. de Tomasi, A. Fioretti, P. Nosbaum, V. M. Akulin, and P. Pillet, Phys. Rev. Lett. **80**, 253 (1998).

[4] S. Westermann, T. Amthor, A. L. de Oliveira, J. Geiglmayr, M. Reetz-Lamour, and M. Weidemüller, Eur. Phys. J. D **40**, 37 (2006).

[5] B. Sun and F. Robicheaux, Phys. Rev. A **78**, 040701 (2008).

[6] J. M. Kondo, L. F. Gon calves, J. S. Cabral, J. Tallant, and L. G. Marcassa, Phys. Rev. A **90**, 023413 (2014).

[7] R. Heidemann, U. Raitzsch, V. Bendkowsky, B. Butscher, R. Löw, L. Santos, and T. Pfau, Phys. Rev. Lett. **99**, 163601 (2007).

[8] E. Urban, T. A. Johnson, T. Henage, L. Isenhower, D. D. Yavuz, T. G. Walker, and M. Saffman, Nat. Phys. **5**, 110 (2009).

[9] A. Gaëtan, Y. Miroshnychenko, T. Wilk, A. Chotia, M. Viteau, D. Comparat, P. Pillet, A. Browaeys, and P. Grangier, Nat. Phys. **5**, 115 (2009).

[10] S. Ravets, H. Labuhn, D. Barredo, L. Béguin, T. Lahaye, and A. Browaeys, Nat. Phys. **10**, 914 (2014).

[11] K. Afrousheh, P. Bohlouli-Zanjani, D. Vagale, A. Mugford, M. Fedorov, and J. D. D. Martin, Phys. Rev. Lett. **93**, 233001 (2004).

[12] C. S. E. van Ditzhuijzen, A. F. Koenderink, J. V. Hernández, F. Robicheaux, L. D. Noordam, and H. B. van Linden van den Heuvell, Phys. Rev. Lett. **100**, 243201 (2008).

[13] D. P. Fahey, T. J. Carroll, and M. W. Noel, Phys. Rev. A **91**, 062702 (2015).

[14] S. E. Anderson, K. C. Younge, and G. Raithel, Phys. Rev. Lett. **107**, 263001 (2011).

[15] T. Pohl, E. Demler, and M. D. Lukin, Phys. Rev. Lett. **104**, 043002 (2010).

[16] B. Yan, S. A. Moses, B. Gadway, J. P. Covey, K. R. A. Hazzard, A. M. Rey, D. S. Jin, and J. Ye, Nature (London) **501**, 521 (2013).

[17] H. Weimer, R. Löw, T. Pfau, and H. P. Büchler, Phys. Rev. Lett. **101**, 250601 (2008).

[18] S. Ji, C. Ates, and I. Lesanovsky, Phys. Rev. Lett. **107**, 060406 (2011).

[19] J. Otterbach, M. Moos, D. Muth, and M. Fleischhauer, Phys. Rev. Lett. **111**, 113001 (2013).

[20] P. Schauss, M. Cheneau, M. Endres, T. Fukuhara, S. Hild, A. Omran, T. Pohl, C. Gross, S. Kuhr, and I. Bloch, Nature (London) **491**, 87 (2012).

[21] D. Petrosyan, Phys. Rev. A **88**, 043431 (2013).

[22] W. Zeller, M. Mayle, T. Bonato, G. Reinelt, and P. Schmelcher, Phys. Rev. A **85**, 063603 (2012).

[23] S. Wüster, C. Ates, A. Eisfeld, and J. M. Rost, New J. Phys. **13**, 073044 (2011).

[24] H. Schempp, G. Günter, S. Wüster, M. Weidemüller, and S. Whitlock, Phys. Rev. Lett. **115**, 093002 (2015).

[25] G. Günter, H. Schempp, M. Robert-de-Saint-Vincent, V. Gavryusev, S. Helmrich, C. S. Hofmann, S. Whitlock, and M. Weidemüller, Science **342**, 954 (2013).

[26] T. Scholak, T. Wellens, and A. Buchleitner, Phys. Rev. A **90**, 063415 (2014).

[27] F. Robicheaux, J. V. Hernández, T. Topçu, and L. D. Noordam, Phys. Rev. A **70**, 042703 (2004).

[28] S. Möbius, M. Genkin, S. Wüster, A. Eisfeld, and J. M. Rost, Phys. Rev. A **88**, 012716 (2013).

[29] A. Eisfeld, S. M. Vlaming, V. A. Malyshev, and J. Knoester, Phys. Rev. Lett. **105**, 137402 (2010).

[30] S. M. Vlaming, V. A. Malyshev, A. Eisfeld, and J. Knoester, J. Chem. Phys. **138**, 214316 (2013).

[31] D. L. Shepelyansky, Phys. Rev. Lett. **73**, 2607 (1994).

[32] J. H. Hoogenraad and L. D. Noordam, Phys. Rev. A **57**, 4533 (1998).

[33] W. Li, I. Mourachko, M. W. Noel, and T. F. Gallagher, Phys. Rev. A **67**, 052502 (2003).

[34] D. J. Griffiths, *Introduction to Quantum Mechanics*, 2nd ed. (Pearson Education, Inc., New Jersey, 2005).